

Inundation Caused by Sea-Level Rise Combined with Land Subsidence

K. Yasuhara¹, S. Murakami² and N. Mimura³

¹Professor Emeritus, Institution of Global Change Adaptation Science, Ibaraki University, Mito, Japan

²Associate Professor, Department of Urban and Civil Engineering, Ibaraki University, Hitachi, Japan

³President, Ibaraki University, Mito, Japan

E-mail: yasuhara@mx.ibaraki.ac.jp

ABSTRACT: As a crucially important issue that Asia-Pacific region residents are currently confronting, this paper treats an increasing probability of unusual and extreme natural disasters that continue as a consequence of climate change, combined with sea-level rise (SLR). The calculated inundation areas in two low-lying regions in Thailand and Japan are visualized using a geographical information system (GIS). Results suggest that the effect of SLR on increasing inundation is more remarkable than that of land subsidence. Therefore, appropriate adaptation measures must be undertaken by the respective regions to avoid the enormous losses and damage from inundation that are expected to derive from the effects of SLR combined with land subsidence.

KEYWORDS: Sea-level rise, Land subsidence, Inundation, Compound disaster

1. INTRODUCTION

Currently, Asia-Pacific region residents are confronting the following circumstances: (1) increased frequency of abnormal weather such as increased torrential downpours has recently become noteworthy; (2) a recently developed climate model has forecast that future typhoons might exhibit increased severity, although the scientific reliability for causality between these extreme events and global warming is not high; and (3) an increasing probability of unusual and extreme natural disasters continues as a consequence of climate change, combined with a sea-level rise (SLR). Particularly, we explore the study of combined phenomena, designated as compounded natural hazards, which are classifiable into two disaster types: those which occur because of the overlap of global warming factors; and those which occur by the overlap of factors that are related to and independent of global warming, which then engender such disasters (Yasuhara, 2009; Yasuhara et al., 2012).

Coastal zones and riverine areas are the residential areas most likely to be influenced by global warming. Especially, seashores in lowland areas would be influenced most if global warming were to raise the typhoon frequency or intensity. Climate factors might cause disasters that are more severe if smaller disasters were to occur concurrently. Figure 1 portrays a disaster that is deemed important and which occurs from overlapping factors. It is designated herein as a complex disaster: a disaster which occurs by overlapping of global warming factors, with factors related to or independent of global warming. Compound geo-disasters are roughly classifiable as disasters related to water (water disasters) or disasters related to soil or ground conditions or behaviors (geological hazards). Unfortunately, knowledge and experience related to geotechnical engineering have remained inadequate to address compound disasters. This paper therefore describes compound geo-disaster phenomena and specifically examines the effects of sea-level rise (SLR) because SLR increases vulnerability and accentuates the impacts of disasters through events such as inundation during severe storm surges and typhoons and sometimes during earthquakes, with increasing probability of compound disasters taking place through a combination of events with and without association with climate change. In addition to such situations, vulnerability from social and human background factors and vulnerability from natural background factors also trigger increases in compound disasters.

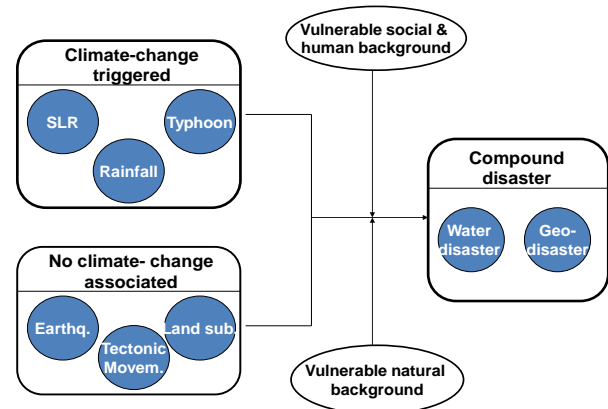


Figure 1 Compound disasters

2. GLOBALLY SCALED INUNDATION CAUSED BY SEA-LEVEL RISE COMBINED WITH LAND SUBSIDENCE

2.1 Inundation Caused by Sea-Level Rise

Three major deltas in the world are shown among the many in Figure 2 (IPCC, 2007): The Nile, Ganges, and Mekong. Those three are designated as the extremely vulnerable coastal deltas. Coastal vulnerability is defined as shown below in Figure 3.

Using the vulnerability index given by Figure 3, Maruyama and Mimura (2010) conducted numerical prediction of the effects of SLR on inundation that can be expected at the end of the 21st century. The results with no adaptation are depicted in Figure 4, indicating that wide areas in Asian regions are inundated by SLR.

2.2 Inundation Caused by SLR Combined with Land Subsidence

The relative vulnerability presented previously in Figure 4 shows no combined effect of SLR with land subsidence. To resolve this gap, an attempt was made to plot the representative locations experiencing severe land subsidence in Figure 5, which presents inundated areas obtained by assuming a sea-level rise to 88 cm at the end of the 21st century for the SRES A1B scenario.



Figure 2 Relative vulnerability of coastal deltas (IPCC WGII, 2007)

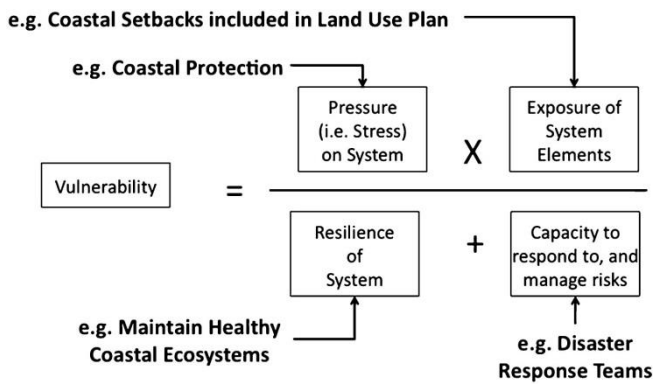


Figure 3 Vulnerability components (from Hay and Mimura, (2010))

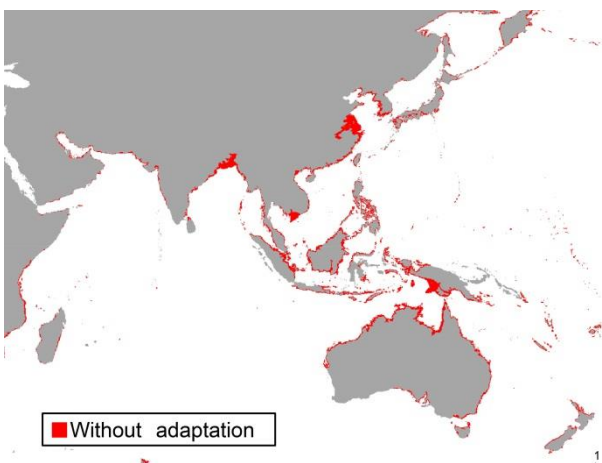


Figure 4 Inundation predictions for 2100 for the SRES A1B scenario with coastal protection for 1/100 storm surges. (dark shows inundation areas) (Maruyama and Mimura, 2010; Mimura, 2013)

Figure 5 shows an inundation area in Southeast Asia as influenced by land subsidence and SLR. This combined effect of land subsidence and SLR is expected to increase relative SLR, which is defined in Figure 6. This in turn engenders increased inundation. Therefore, we should carry out both precise predictions of time-dependent variations of SLR and land subsidence at least to 2100.

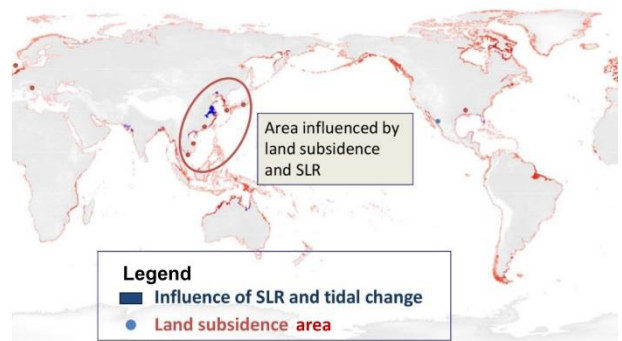


Figure 5 Inundation areas combined SLR and tidal change with land subsidence

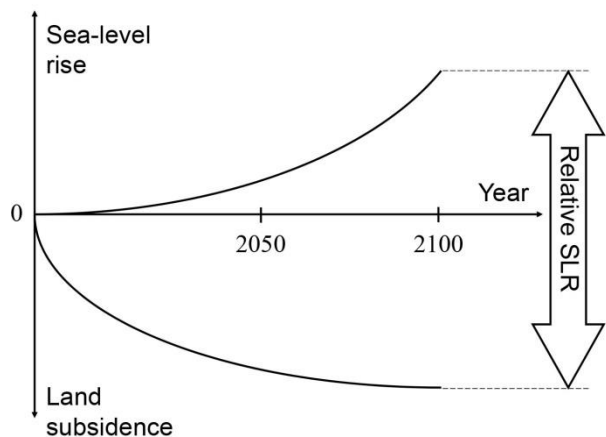


Figure 6 Definition of relative sea-level rise (SLR)

3. PREDICTION OF SLR AND LAND SUBSIDENCE

3.1 Scenario of SLR

Several scenarios show SLR variation over time. Figure 7 presents a typical variation of SLR with elapsed time in 2100 (IPCC, 2007), which was adopted here for numerical prediction for inundation induced by combination of SLR with land subsidence.

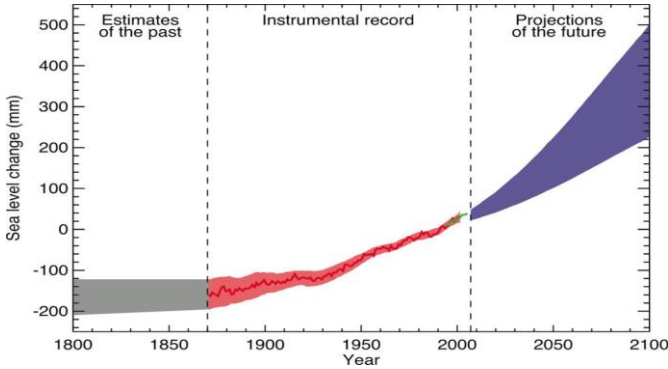


Figure 7 Typical variation of SLR with elapsed time in 2100 (IPCC, 2007)

3.2 Observational Procedure for Predicting Land Subsidence

To predict variations of land subsidence over time, the observational methodology proposed by Murakami et al. (2003) was adopted. The methodology is illustrated schematically in Figure 8, showing settlement vs. elapsed time relations starting from an arbitrary time given by

$$\delta S_i = S_{p0} \{1 - \exp(-C_R \delta t_i)\} \tag{1}$$

where S_{p0} is the residual settlement expected from the present time until the termination of subsidence under the assumption that the groundwater variation is maintained as observed now and assuming that C_R is a parameter corresponding to the settlement strain rate. Those two parameters are given respectively as shown below.

$$S_{p0} = S_f \frac{8}{\pi^2} \exp\left(-\frac{T_{v0}}{4}\right) \tag{2}$$

$$C_R = \frac{\pi^2}{4} \frac{c_v}{H_d^2} \tag{3}$$

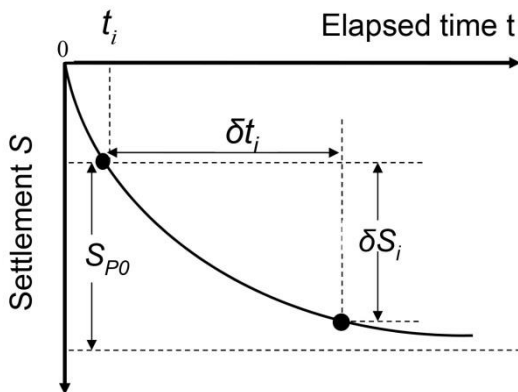


Figure 8 Observational prediction procedure of land subsidence

The procedures shown in Figure 8 and described in Eq. (1) – Eq. (3) are based on the solution of the Terzaghi’s one-dimensional theory of consolidation for saturated soils given as the following.

$$\frac{\partial u}{\partial t} = c_v \frac{\partial^2 u}{\partial z^2} \tag{4}$$

Therein, c_v included in Eq. (4) is the coefficient of consolidation. The two parameters S_{p0} and C_R given by Eqs. (1b) and (1c) in the observational methodology were determined Based on results of settlement vs. time relations observed before the start of prediction using the nonlinear least squares method (Murakami et al., 2003; Murakami et al., 2005; Murakami and Yasuhara, 2011, see Appendix I).

4. CASE STUDY: CHAO PHRAYA DELTA, THAILAND

4.1 Outline of the Case Study

Deltas such as the Chao Phraya Delta, Red River Delta and Mekong River Delta included in Figure 2 are “Mega Deltas.” An IPCC report (2007) described that Mega Deltas will be most vulnerable to natural disasters induced by global climate change because Mega Deltas are located in very low land in coastal regions that will be affected directly by sea-level rise caused by global warming. Already, land subsidence has occurred in many Mega Deltas. A typical region that has been affected by both SLR and land subsidence is the Chao Phraya Delta in Thailand, which this study examines.

To assess the influence of the dual impacts of sea-level rise and land subsidence on inundated areas of the Chao Phraya Delta, the future situation of land subsidence in 2100 has been predicted using a method of reliable land subsidence mapping based on observations of settlement proposed by Murakami et al. (2005, 2006). The future elevation model in the objective regions was made by incorporating the present elevation model and the predicted land subsidence into GIS. To investigate the influence of dual impacts of both sea-level rise and land subsidence on inundation area in the Chao Phraya Delta, a hazard map of the inundation area has been presented. The hazard map shows the approximately 1,000 km² inundation area caused by dual impacts of sea-level rise and land subsidence which will be shown later.

4.2 Present Situation of Land Subsidence in Chao Phraya

There are approximately 748 observation locations for monitoring settlement during 1996–2003 in Chao Phraya Delta, some of which are shown in Figure 9. The present situation of land subsidence in the objective regions can be elucidated using the time-series records of settlement. A map of land subsidence has been produced using reliable land subsidence mapping using a spatial interpolation procedure based on geostatistics proposed by Murakami, Yasuhara and Suzuki (2005), and Murakami and Yasuhara (2006) in this study. The mapping method can show not only the distribution of expected settlement but also the distribution of estimated standard deviations based on the spatial correlation relations of settlement. The interpolation method is based on Kriging, a spatial interpolation method. It is assumed that estimation at a location can be expressed as a linear weighted summation of the observations. Figure 10 shows interpolated results of the distribution of land subsidence in the objective region during 1996–2003. The estimated settlement is drawn as contour lines. The estimated standard deviations are shown as raster data. The map shows that severe land subsidence has taken place in Samut Prakarn, the middle of Samut Sakhon, and the north of Pathum Thani.

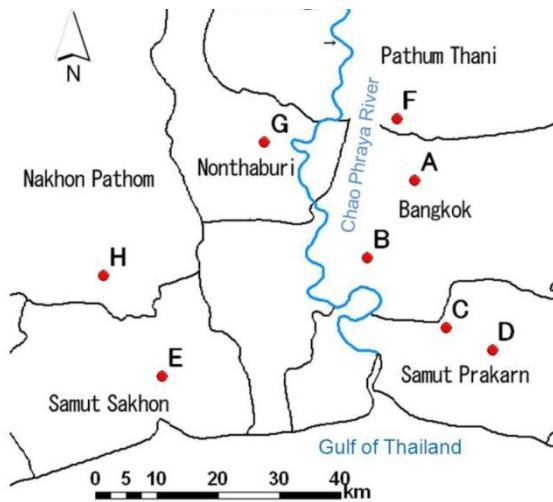


Figure 9 Locations observed for land subsidence in Chao Phraya

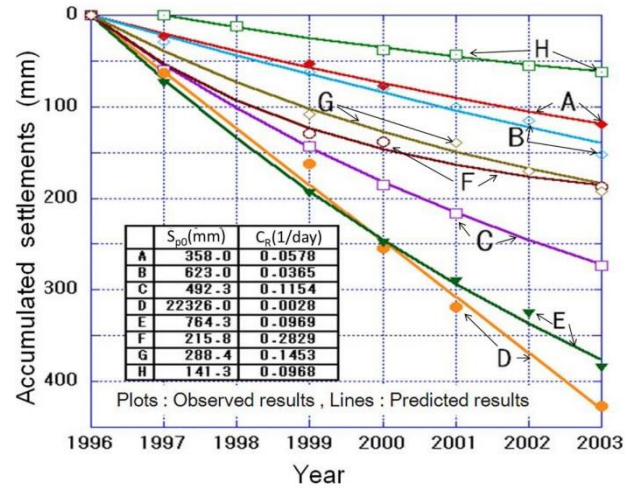


Figure 11 Comparison between observed and predicted settlement vs. elapsed time relations

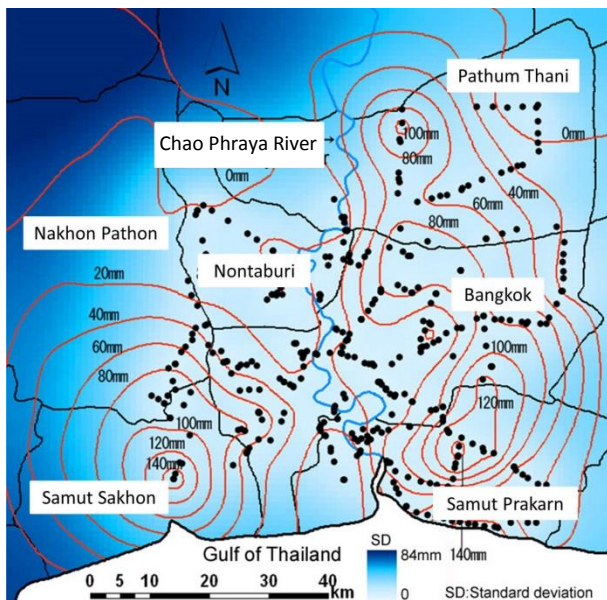


Figure 10 Contour lines of land subsidence in Chao Phraya Delta

4.3 Future Conditions of Land Subsidence

To investigate the future conditions of land subsidence in the objective region, an observational method for land subsidence originally proposed by Murakami et al. (2005) was used. The method assumes that the cumulative settlement subjected to seasonal changes of ground water level can be expressed as the similar curve of Terzaghi's one-dimensional consolidation theory. The cumulative settlement, S_i , after elapsed time, t_i , from the beginning of observation can be predicted using Eq. (1).

For the investigation of the applicability of the method to future settlement prediction in the objective region, the method has been applied to eight representative locations (A–H) shown in Figure 9. Figure 11 compares the observed and predicted results of cumulative settlement in the represented locations. They show good agreement with observed and predicted results.

The future conditions of land subsidence in 2100 were predicted using a method of reliable land subsidence. Future cumulative settlement at all observation locations has been predicted using Eq. (1). The future land subsidence map has been represented also using the proposed method for a reliable land subsidence mapping.

Figure 12 shows a future situation of land subsidence that will occur during 2001–2100. The map in Figure 12 shows the estimated standard deviation, which depends on both the spatial interpolation error and the future prediction. The map exhibits severe settlement in the middle-eastern parts of Samut Prakarn and the northern side of Samut Sakhon. Therefore, the severe land subsidence will move to the northern side in Samut Sakhon, although severe land subsidence in the northern side of Pathum Thani will become small. Comparing the land subsidence map of the present situation with that of the future situation, the distribution of estimated standard deviation in the map of the future situation is larger than the map of future situation because the estimated standard deviation of the future land subsidence map depends on both the spatial interpolation error and future prediction one. Therefore, it is important to investigate dual-hazards caused by both sea-level rise and land subsidence to incorporate the estimation error attributable to both spatial interpolation and future predictions.

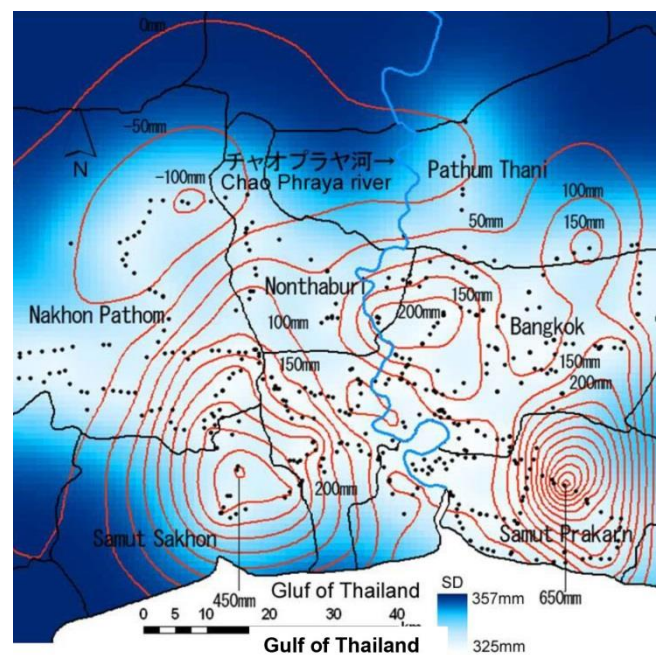


Figure 12 Contour map of the interpolated future land subsidence

4.4 Assessing the Influence of Dual Impacts of SLR and Land Subsidence on Inundation Areas

To assess the influence of dual impacts of sea-level rise attributable to global warming and land subsidence on inundation area in the Chao Phraya Delta, GIS-aided spatial analysis was conducted based on the predicted result of future land subsidence in 2100, as shown in Figure 12. The inundation area, defined as the region with ground level under the sea-level in the future situation, was calculated from the present ground level considering future land subsidence. SLR in this study was assumed as 59 cm according to an IPCC report (2007).

Figures 13(a), 13(b), and 13(c) show calculated results of inundation caused by SLR in 2100. Figure 13(a) presents inundation regions considering SLR only. For the impact of SLR only, the coastal regions in Samut Sakhon, Bangkok and Samut Prakarn and the middle region of Bangkok are inundated. Figure 13(b) shows inundated regions considering dual impacts of SLR and land subsidence. Figure 13(b) shows that inundated regions tend to expand by adding consideration of future land subsidence to the impact of SLR. Particularly, it is marked in expanding the inundated areas in the middle region of Samut Prakarn where severe land subsidence will occur. Finally, Figure 13(c) depicts inundated regions caused by dual impacts of sea-level rise and land subsidence considering estimation error caused by spatial interpolation and land subsidence prediction. The map in Figure 13(c) shows that the inundated region expands more markedly over 60% than in the case of dual impacts being considered, which is shown in Figure 13(b), without consideration of estimation error, as shown in Table 1.

Table 1 Comparison of inundation area for three cases

	(a)	(b)	(c)
Areas of inundation (km ²)	634	779	1269

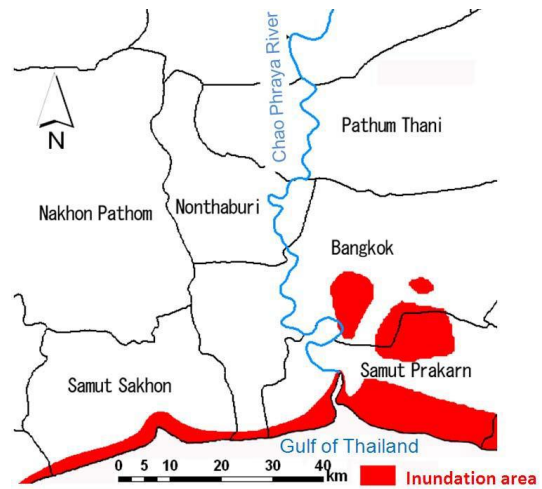
Overall, the results show that it is important for estimating precisely the inundated region in the future situation affected by global warming to consider the impacts not only of sea-level rise but also land subsidence, particularly through devotion of careful attention to the estimation error.

5. CASE STUDY IN ECHIGO PLAIN, NIIGATA, JAPAN

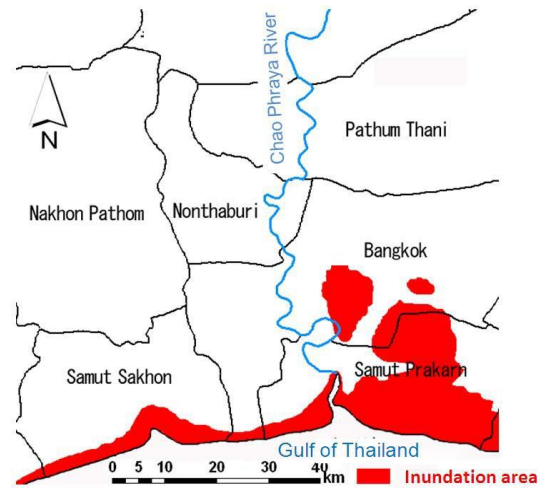
5.1 Outline of the Objective Region, Echigo plain

Land subsidence in Japan has become calmer because of the governmental regulation of groundwater abstraction since around 1963. Issues have emerged in relation to recovery of groundwater level (GWL), such as floating of underground structures and increasing potential of liquefaction in sandy deposits, particularly in urban areas which are induced by rise in GWL. Some regions have been adversely affected by marked land subsidence. The Echigo plain in Niigata (see Figure 14, which shows areas that experienced severe land subsidence in 2013 (MOE Report, 2014). We designate the Echigo plain in the current paper, although this area is also called the “Niigata plain.” The Echigo plain existing on the thick alluvial deposits including Niigata City, the prefectural capital, is an important food production area in Japan and maintains ecological richness, as represented by the inhabitation of wild birds.

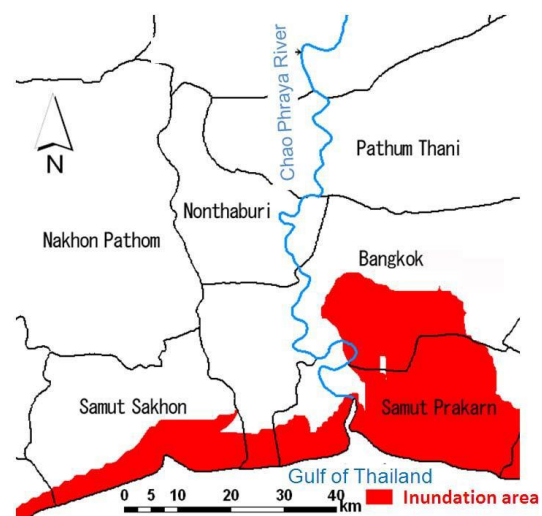
From a historical perspective, land subsidence took place in Echigo plain mainly because of abstraction of groundwater for agricultural purposes and exploitation of oil and natural gas for industrial purposes. Very recently, people in Echigo have had about 2 cm of land subsidence annually because of the use of water for melting heavy snow in winter. The widely spreading thick alluvial deposits are responsible for land subsidence, which will increase inundation and flood damage in the plain.



(a) Inundation area caused by only sea-level rise



(b) Inundation area caused by sea-level rise and land subsidence



(c) Inundation area caused by sea-level rise and land subsidence with estimation error

Figure 13 Predicted inundation areas in the Chao Phraya Delta



Figure 14 Location of Niigata Prefecture in Japan

5.2 Prediction of Land Subsidence

Based on the same procedures as adopted in the case in the Chao Phraya Delta, we started prediction of the variations of land subsidence over time by the end of the 21st century. Figure 15 depicts three examples of variations of measured and predicted settlement with elapsed time.

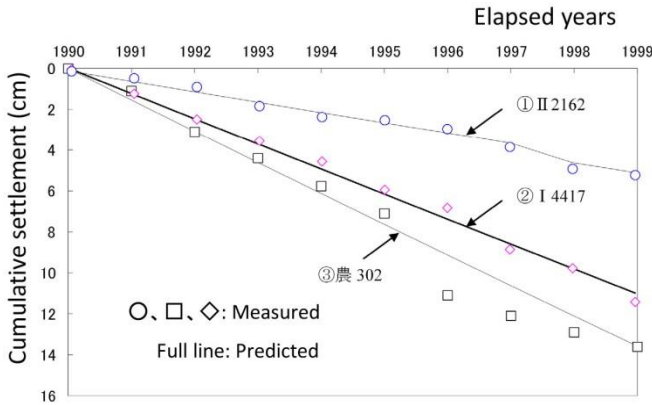


Figure 15 Settlement vs. elapsed time relations for three locations

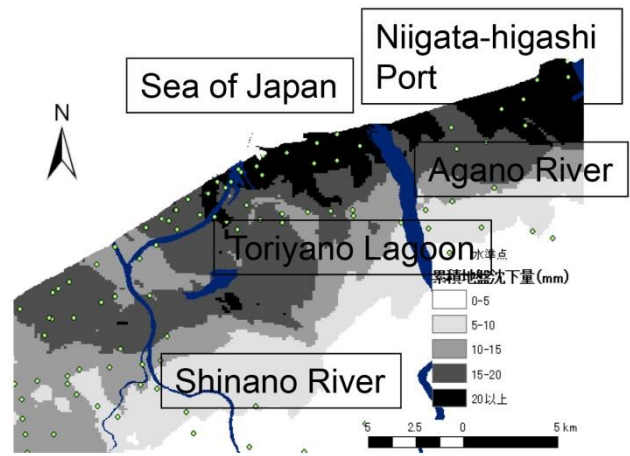
Using predicted settlement obtained by adopting the proposed observational method for 168 locations through the Echigo plain including three examples shown in Figure 16. As obtained using records of settlement for the last five years shown in Figure 16(a) and distribution of predicted settlement at 2100 is shown in Figure 16(b).

5.3 Prediction of Inundation

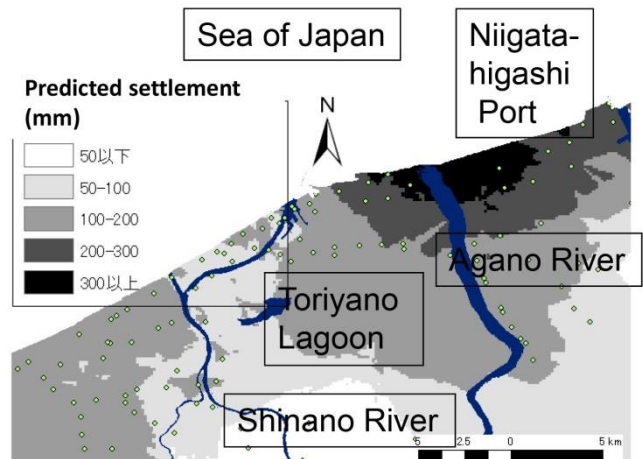
The scenario of SLR necessary for dual effects on inundation was the same as that adopted in Chapter 4 for the case study in Chao Phraya Delta, which was based on Figure 7. The relative SLR defined in Figure 6, which combines both effects of land subsidence and SLR, was adopted to demonstrate the severity of inundation in the same manner as used in the case for Chao Phraya Delta. An example for a set of variations of predicted SLR and land subsidence with elapsed time (in year) is presented in Figure 17.

Variations of land subsidence with elapsed time were obtained by extrapolating data obtained during 2001 through 2005 statistically using Eq. (1). Results calculated using the same procedure for 168 locations are presented in Figure 18 using Geographical Information System (GIS) for cases with and without SLR considered in addition to land subsidence. Here in Figure 18, special attention should be devoted to the fact that the inundated areas are assumed to be equivalent to the difference between altitude and relative SLR defined in Figure 6. It can be emphasized from the

results in Figure 18 that the effect of SLR on increasing inundation is more remarkable than that of land subsidence. This tendency is almost identical to that for the Chao Phraya Delta in Thailand, both of which are typical lowland areas in the Asia-Pacific region.



(a) Cumulative settlement (2001–2005)



(b) Predicted cumulative settlement (2100)

Figure 16 Observed and predicted land subsidence in Echigo plain, Niigata, Japan

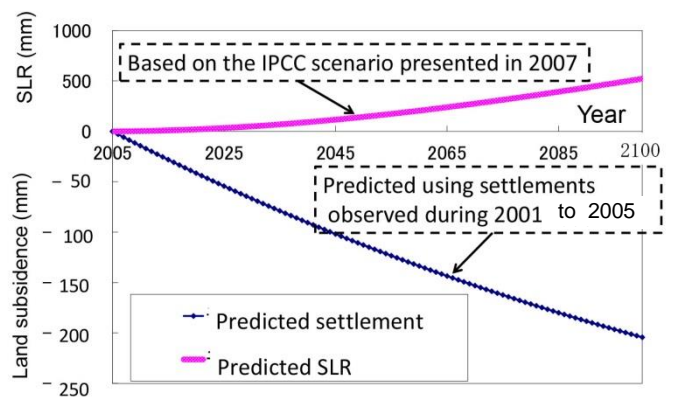
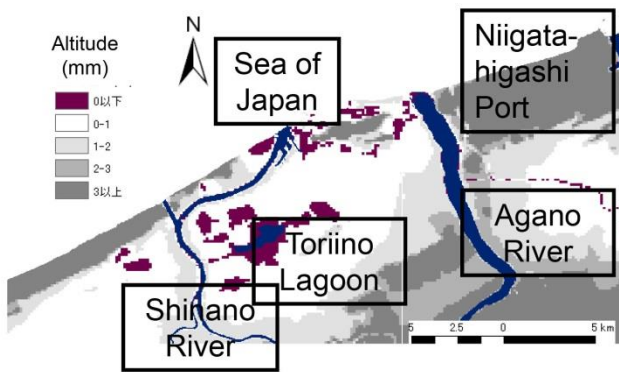
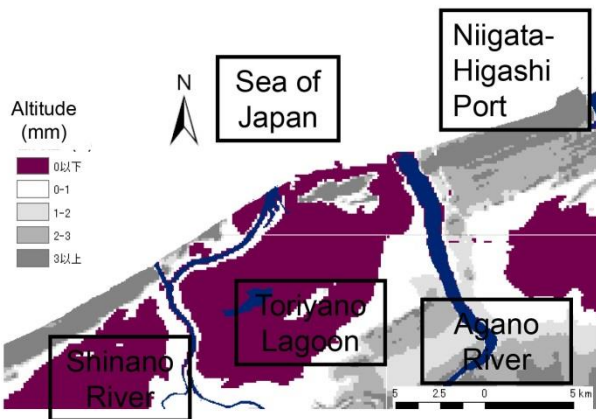


Figure 17 Set of variations of predicted SLR and land subsidence with elapsed time (in year)



(a) Land subsidence only considered



(b) Both land subsidence and SLR considered

Figure 18 Distribution of predicted inundation areas in the cases with and without SLR combined with land subsidence

Table 2 presents inundated areas for cases with land subsidence only, SLR only, and both land subsidence and SLR being considered. It can be inferred from Figure 18 and Table 2 that the effect of SLR on increasing inundation is more remarkable than that of land subsidence. Almost half of the Echigo plain will be inundated with no adaptation against increasing SLR and land subsidence. This tendency resembles that observed for the Chao Phraya Delta.

Table 2 Inundated area for cases with and without land subsidence and SLR considered

Case for prediction	Inundated area (%)
Land subsidence only considered	7.5
SLR only considered	47.6
Both land subsidence and SLR considered	49.0

6. CONCLUSION

This paper describes the increasing probability of inundation as a consequence of SLR combined with land subsidence. The calculated inundation areas in two objective regions in Japan and Thailand are depicted using a geographical information system (GIS) for visualization. Results show the following.

- i) The effect of SLR on increasing inundation is more remarkable than that of land subsidence. This tendency is apparent for the Chao Phraya Delta in Thailand and the Echigo plain in Japan, which are typical lowland areas in Asia-Pacific regions.
- ii) Appropriate adaptation measures must be undertaken by the respective regions to avoid enormous losses and damage from inundation, which are expected to derive from the combined effects of land subsidence and SLR.

Acknowledgements:

This research was partly supported by a Grant-in-Aid for Scientific Research from the Ministry of Education, Culture, Sports, Science and Technology (FY2014–FY2017, Project No. 26281055), Japan and the Environment Research and Technology Development Fund (S-8) of the Ministry of Environment, Japan (FY2010–FY2014). This support is greatly appreciated. We extend our sincere thanks to colleagues who participated in these projects.

7. REFERENCES

- Hay J. E., and Mimura, N. (2010). “The changing nature of extreme weather and climate events: risks to sustainable development”, *Geomat Nat Hazards Risk* Vol. 1(1), pp. 3-18.
- IPCC (2007). “Climate Change 2007 – The Physical Science Basis: Working Group I Contribution to the Fourth Assessment Report of the IPCC” Cambridge University Press, Cambridge and New York.
- Maruyama, Y., and Mimura, N. (2010). “Global assessment of climate change impacts on coastal zones with combined effects of population and economic growth”, *Selected Papers of Environmental Systems Research, JSCE 38*, pp. 255-263 (in Japanese).
- Mimura, N. (2013). “Sea-level rise caused by climate change and its implications for society – Review”, *Proc. Jpn. Acad., Ser. B* 89, No. 7, pp. 281-301.
- Murakami, S., Yasuhara, K., and Mochizuki, N. (2003). “An observational prediction of land subsidence applied for GIS”, *Journal of Japanese Association of Groundwater Hydrology*, Vol. 45, No. 3, pp. 391-407, (in Japanese).
- Murakami, S., Yasuhara, K., and Suzuki, K. (2005). “Reliable Land Subsidence Mapping by a Geostatistical Spatial Interpolation Procedure.” *Proc. 16th Int. Conf. Soil Mechanics and Geotech. Eng.* Vol. 4, pp. 2829-2832.
- Murakami, S., and Yasuhara, K. (2011). “Inundation due to global warming and land subsidence in Chao Phraya Delta”, *Proc. 14th Asian Reg. Conf. SMGE*, Vol. 1 (CD-ROM).
- Takei, S., Yasuhara, K., Murakami, S., Suzuki, K., and Komine, H. (2009). “Influence of sea-level rise on inundation in the land subsidence area”, *Proc. Eighth Symp. on Environmental Geotechnology*, Vol. 1, pp. 385-388 (in Japanese).
- Yasuhara, K. (2009). “Global warming and compound geo-disasters”, *Journal of Japanese Geotechnical Society*, Vol. 57-4 (615), pp. 1-6 (in Japanese).
- Yasuhara, K., Komine, H., Murakami, S., Chen, G., Mitani, Y., Duc, D. M. (2012). “Effects of climate change on geo-disasters in coastal zones and their adaptation”, *Geotextiles and Geomembranes*, Vol. 30, pp. 24-34.

APPENDIX I: OBSERVATIONAL PREDICTION OF LAND SUSDENCE

A first attempt was made to predict relations of future settlement versus elapsed time based on land subsidence-time records previously measured at locations in Bangkok in Thailand and Niigata Plain in Japan. However, because the method was described already in earlier reports (Murakami et al., 2003, 2005, 2011), following is a brief procedural review.

Figure 8 schematically presents a settlement set and relation of GWL against time. Although the external load given by Δh (fluctuation in GWL) varies with time, here the cumulative settlement at every cycle of GWL fluctuation is assumed to be governed by conventional one-dimensional consolidation theory as

$$\frac{\partial u}{\partial \tau} = c_v \frac{\partial^2 u}{\partial z^2}, \tag{A1}$$

where τ is the time from starting GWL fluctuation, u denotes the excess pore pressure, and c_v represents the coefficient of consolidation. The general solution for drainage top and bottom (drainage distance is H_d) is given as

$$\Sigma = \Sigma_f \left\{ 1 - \sum_{n=1}^{\infty} \frac{2}{a_n^2} \exp(-a_n^2 T_v) \right\}, \tag{A2}$$

$(a_n = \frac{2n-1}{2} \pi ; n=1,2,3,\dots)$

where Σ stands for the settlement from starting GWL fluctuation, Σ_f represents the final settlement, and T_v denotes the time factor defined as shown below.

$$T_v = \frac{c_v}{H_d^2} \tau \tag{A3}$$

When we consider the interval between two time factors of T_{v0} and T_{vi} , which respectively relate to Σ_0 and Σ_i , the difference settlement S_i yields the following.

$$S_i = \Sigma_i - \Sigma_0 = \Sigma_f \cdot \sum_{n=1}^{\infty} \left[\frac{2}{a_n^2} \exp(-a_n^2 T_{v0}) \left(1 - \exp\{-a_n^2 (T_{vi} - T_{v0})\} \right) \right] \tag{A4}$$

Using Eq. (3), $T_{vi} - T_{v0}$ in Eq. (4) can be expressed as

$$T_{vi} - T_{v0} = \frac{c_v}{H_d^2} (\tau_i - \tau_0) = \frac{c_v}{H_d^2} t_i, \tag{A5}$$

where t_i is time from the beginning of measuring settlement. By neglecting the difference in inherent values after the second order in the consolidation theory solution, Eq. (4) leads to the following.

$$S_i = \Sigma_f \frac{8}{\pi^2} \exp\left(-\frac{\pi^2}{4} T_{v0}\right) \left\{ 1 - \exp\left(-\frac{\pi^2}{4} \frac{c_v}{H_d^2} t_i\right) \right\} \tag{A6}$$

Therein, S_i is the cumulative settlement from the beginning of measuring settlement to t_i . Let us here assume that

$$S_{p0} = \Sigma_f \frac{8}{\pi^2} \exp\left(-\frac{\pi^2}{4} T_{v0}\right), C_R = \frac{\pi^2}{4} \frac{c_v}{H_d^2}, \tag{A7}$$

where S_{p0} is the residual settlement expected from the present time until the termination of subsidence under the assumption that the groundwater variation is maintained at the level observed now and that C_R is a parameter corresponding to the settlement strain rate. Substitution of Eq. (A7) into Eq. (A6) yields

$$S_i = S_{p0} \{1 - \exp(-C_R \cdot t_i)\} \tag{A8}$$

As the general form instead of Eq. (A8), suitable for an arbitrary time, we have the following.

$$S = S_{p0} \{1 - \exp(-C_R \cdot t)\} \tag{A9}$$

The concrete values of two parameters are given by Eq. (A7). These are determined using the nonlinear least squares method which should satisfy the following (Murakami et al., 1998)

$$\frac{\partial F_1}{\partial S_{p0}} = 0, \quad \frac{\partial F_1}{\partial C_R} = 0, \tag{A10}$$

where F_1 is given as

$$F_1 = \sum_{i=1}^n \left[S_i^m - S_{p0} \{1 - \exp(-C_R \cdot t_i)\} \right]^2, \tag{A11}$$

in which S_i^m is the observational settlement at t_i . A family of data of S_{p0} and C_R for typical locations at the objective area was adopted for forecasting future settlement variation with elapsed time through previously recorded values of land subsidence.